International Communications in Heat and Mass Transfer 37 (2010) 873–880

Contents lists available at ScienceDirect

International Communications in Heat and Mass Transfer

journal homepage: www.elsevier.com/locate/ichmt

Heat and mass transfer by natural convection in a doubly stratified non-Darcy micropolar fluid ☆

D. Srinivasacharya, Ch. RamReddy

Department of Mathematics, National Institute of Technology, Warangal-506004, Andhra Pradesh, India

ARTICLE INFO

Available online 3 June 2010

Keywords:
Natural convection
Non-Darcy porous medium
Micropolar fluid
Thermal Stratification
Solutal Stratification
Heat and mass transfer

ABSTRACT

Natural convection heat and mass transfer along a vertical plate embedded in a doubly stratified micropolar fluid saturated non-Darcy porous medium is presented. The governing nonlinear equations are solved numerically using the Keller-box method. The effects of physical parameters on velocity, microrotation, temperature, concentration, local skin friction and wall couple stress coefficient, heat and mass transfer coefficients are illustrated graphically and in tabular form. The results of convection in a micropolar fluid along a vertical plate are obtained as a special case from the present analysis and are found to be in good agreement with the previously published results.

1. Introduction

Natural convection flow is caused by buoyancy forces which arise from density differences in a fluid. These density differences are consequence of temperature gradients within the fluid. Natural convection flows in a fluid saturated porous media are of great interest because of their applications in design of chemical processing equipment, formation and dispersion of fog, distributions of temperature and moisture over agricultural fields, grain storage systems, heat pipes, packed microsphere insulation, distillation towers, ion exchange columns, subterranean chemical waste migration, solar power absorbers etc. A number of studies have been reported in the literature focusing on the problem of combined heat and mass transfer in porous media. Nield [1] made the first attempt to study the stability of convective flow in horizontal layers with imposed vertical temperature and concentration gradients. This was followed by Khan and Zebib [2] in the study of flow stability in a vertical porous layer. An analysis of the mass transfer effect on the free convective transport of a viscous fluid past an infinite vertical porous plate was carried out by Soundalgekar [3]. The analysis of convective heat and mass transfer in a porous medium with the inclusion of non-Darcian effects has also been a matter of study in recent years. The inertia effect is expected to be important at a higher flow rate and it can be accounted for through the addition of a velocity squared term in the momentum equation, which is known as the Forchheimer's extension. Several researchers have studied natural convection heat and mass transfer in porous medium by considering Forchheimer's extension. A detailed review of convective heat transfer in Darcian and Non-Darcian porous media can be found in the book by Nield and Bejan [4].

The study of non-Newtonian fluid flows has gained much attention by the researchers because of its applications in biology, physiology, technology and industry. In addition, the effects of heat and mass transfer in non-Newtonian fluid saturated porous media also have great importance in engineering applications like the thermal design of industrial equipment dealing with molten plastics, polymeric liquids, foodstuffs, or slurries. Several investigators have extended many of the available convective heat and mass transfer in fluid saturated porous media problems to include the non-Newtonian effects. Many of the non-Newtonian fluid models, describe the nonlinear relationship between stress and the rate of strain. But the micropolar fluid model introduced by Eringen [5] exhibits some microscopic effects arising from the local structure and micro motion of the fluid elements. Further, they can sustain couple stresses and include classical Newtonian fluid as a special case. The model of micropolar fluid represents fluids consisting of rigid, randomly oriented (or spherical) particles suspended in a viscous medium where the deformation of the particles is ignored. Micropolar fluids have been shown to accurately simulate the flow characteristics of polymeric additives, geomorphological sediments, colloidal suspensions, haematological suspensions, liquid crystals, lubricants etc. The main advantage of using micropolar fluid model compared to other non-Newtonian fluids is that it takes care of the rotation of fluid particles by means of an independent kinematic vector called the microrotation vector. The mathematical theory of equations of micropolar fluids and applications of these fluids in the theory of lubrication and porous media are presented by Lukaszewicz [6]. The heat and mass transfer in micropolar fluids in porous media have received less attention despite important applications in emulsion filtration, polymer gel dynamics in packed beds, petroleum and

☆ Communicated by W.J. Minkowycz.
E-mail addresses: dsrinivasacharya@yahoo.com, dsc@nitw.ac.in (D. Srinivasacharya).

0735-1933/$ – see front matter © 2010 Elsevier Ltd. All rights reserved.
doi:10.1016/j.icheatmasstransfer.2010.05.001

Nomenclature

A	Slope of ambient temperature
b	Forchheimer constant (Geometric)
B	Slope of ambient concentration
$\mathcal{B}$	Buoyancy ratio
C	Concentration
C_w	Wall concentration
C_f	Skin friction coefficient
$C_{\infty,0}$	Ambient concentration
D	Solutal diffusivity
Da_L	Darcy number
f	Reduced stream function
Fs	Forchheimer number
g	Dimensionless microrotation
g^*	Gravitational acceleration
Gr_L	Thermal Grashof number
$\mathcal{J}$	Dimensionless micro-inertia density
j	Micro-inertia density
k	Thermal conductivity
L	Length of the plate
M_w	Dimensionless wall couple stress
m_w	Wall couple stress
N	Coupling number
$\overline{Nu}$	Average Nusselt number
Nu_x	Local Nusselt number
Pr	Prandtl number
Sc	Schmidth number
$\overline{Sh}$	Average Sherwood number
Sh_x	Local Sherwood number
T	Temperature
T_w	Wall temperature
$T_{\infty,0}$	Ambient temperature
U_*	Characteristic velocity
u,v	Darcian velocity components in x and y directions
x,y	Coordinates along and normal to the plate
α	Thermal diffusivity
β_T,β_C	Coefficient of thermal and solutal expansion
γ	Spin-gradient viscosity
δ_T,δ_C	Thermal and Solutal boundary layer thickness
η	Pseudo-similarity variable
θ	Dimensionless temperature
ϕ	Dimensionless concentration
κ	Vortex viscosity
λ	Dimensionless spin-gradient viscosity
μ	Dynamic viscosity
ν	Kinematic viscosity
ξ	Dimensionless streamwise coordinate
ρ	Density of the fluid
τ_w	Wall shear stress
ψ	Stream function
ω	Component of microrotation
$\varepsilon_1,\varepsilon_2$	Thermal and Solutal stratification parameter

Subscripts

w	Wall condition
∞	Ambient condition
C	Concentration
T	Temperature

Superscript

$'$	Differentiation with respect to η

lubrication flows in porous wafers. Free convection boundary layer flow of a micropolar fluid from a vertical flat plate is examined by Rees and Pop [7]. They solved the governing non-similar boundary layer equations numerically using the Keller-box method for a range of values of micropolar fluid parameters. Hassanien et al. [8] have considered natural convection flow of micropolar fluid along a vertical and a permeable semi-infinite plate embedded in a porous medium. They obtained a nonsimilarity solution for the case of uniform heat flux and used a finite-difference scheme to solve the system of transformed governing equations. The problem of fully developed natural convection heat and mass transfer of a micropolar fluid between porous vertical plates with asymmetric wall temperatures and concentrations is analyzed by Abdulaziz and Hashim [9]. They presented an analytic solution to the resulting boundary value problem by the homotopy analysis method (HAM) and profiles for velocity and microrotation are presented for a range of values of the Reynolds number and the micropolar parameter.

Stratification of fluid arises due to temperature variations, concentration differences or the presence of different fluids. The analysis of natural convection in a doubly stratified medium is a fundamentally interesting and important problem because of its broad range of engineering applications. The applications include heat rejection into the environment such as lakes, rivers and the seas; thermal energy storage systems such as solar ponds and heat transfer from thermal sources such as the condensers of power plants. Although the effect of stratification of the medium on the heat removal process in a fluid is important, very little work has been reported in the literature. Murthy et al.[10] have analyzed the effect of double stratification on double diffusive natural convection from a vertical impermeable flat plate in non-Darcy porous media with the constant heat and mass flux conditions at the wall using similarity solution technique. Later, Lakshmi Narayana and Murthy [11] have analyzed the natural convection heat and mass transfer from a vertical surface embedded in a doubly stratified non-Darcy porous medium. They assumed that the wall temperature and concentration are constants and the medium is linearly stratified with respect to both temperature and concentration in the vertical direction. A mathematical model is presented for the two-dimensional, steady, incompressible, laminar free convection flow boundary layer flow over a continuously moving plate immersed in a thermally-stratified high-porosity non-Darcian porous medium by Anwar Beg et al. [12]. Recently, Cheng [13] considered the combined heat and mass transfer in natural convection flow from a vertical wavy surface in a power-law fluid saturated porous medium with thermal and mass stratification.

The main purpose of the present investigation is to study the natural convection heat and mass transfer along a vertical plate in a micropolar fluid saturated non-Darcy porous medium. A numerical solution using the Keller-box method [14] is obtained. The effects of micropolar parameter, Forchheimer number, thermal and mass stratification parameters on the physical quantities of the flow are analyzed. The results are compared with relevant results in the existing literature and are found to be in good agreement.

2. Mathematical formulation

Consider the natural convection heat and mass transfer along a vertical plate of length L embedded in a doubly stratified non-Darcy micropolar fluid. Assume that the fluid and the porous medium have constant physical properties. The fluid flow is moderate and the permeability of the medium is low so that the Forchheimer flow model is applicable and the boundary effect is neglected. The flow is steady, laminar, two-dimensional and the fluid and the porous medium are in local thermodynamical equilibrium. Choose the coordinate system such that x-axis is along the vertical plate and y-axis normal to the plate. The plate temperature is T_w and concentration is C_w and are assumed to be constants. The ambient medium is assumed to be vertically and linearly stratified with respect to both temperature and concentration in the form $T_\infty(x) = T_{\infty,0} + Ax$ and $C_\infty(x) = C_{\infty,0} + Bx$ respectively, where A and B are constants and varied to alter the intensity of stratification in the medium. The values of T_w and C_w are assumed to be greater than the ambient temperature $T_{\infty,0}$ and concentration $C_{\infty,0}$ at any arbitrary reference point in the medium (inside the boundary layer).

Using the Boussinesq and boundary layer approximations, the governing equations for the micropolar fluid are given by

$$\frac{\partial u}{\partial x} + \frac{\partial v}{\partial y} = 0 \tag{1}$$

$$\rho\left(u\frac{\partial u}{\partial x} + v\frac{\partial u}{\partial y}\right) = (\mu+\kappa)\frac{\partial^2 u}{\partial y^2} + \kappa\frac{\partial \omega}{\partial y} + \rho g^*(\beta_T(T-T_\infty) + \beta_C(C-C_\infty)) - \frac{\mu}{K_p}u - \frac{\rho b}{K_p}u^2 \tag{2}$$

$$\rho j\left(u\frac{\partial \omega}{\partial x} + v\frac{\partial \omega}{\partial y}\right) = \gamma\frac{\partial^2 \omega}{\partial y^2} - \kappa\left(2\omega + \frac{\partial u}{\partial y}\right) \tag{3}$$

$$u\frac{\partial T}{\partial x} + v\frac{\partial T}{\partial y} = \alpha\frac{\partial^2 T}{\partial y^2} \tag{4}$$

$$u\frac{\partial C}{\partial x} + v\frac{\partial C}{\partial y} = D\frac{\partial^2 C}{\partial y^2} \tag{5}$$

where u and v are Darcian velocity components in x and y directions respectively, ω is the component of microrotation whose direction of rotation lies in the xy-plane, T is the temperature, C is the concentration, g^* is the acceleration due to gravity, ρ is the density, b is the Forchheimer constant, K_p is the permeability, μ is the dynamic coefficient of viscosity, β_T is the coefficient of thermal expansion, β_C is the coefficient of solutal expansions, κ is the vortex viscosity, j is the micro-inertia density, γ is the spin-gradient viscosity, α is the thermal diffusivity and D is the solutal diffusivity of the medium.

The boundary conditions are

$$u = 0, v = 0, \omega = -n\frac{\partial u}{\partial y}, T = T_w, C = C_w \quad at \quad y = 0 \tag{6a}$$

$$u = 0, \omega = 0, T = T_\infty(x), C = C_\infty(x) \quad as \quad y \to \infty \tag{6b}$$

where k is the thermal conductivity of the fluid, the subscripts w, $(\infty,0)$ and ∞ indicate the conditions at the wall, at some reference point in the medium and at the outer edge of the boundary layer respectively and n is a constant such that $0 \le n \le 1$. Generally, when $n = 0$, Eq. (6a) yields $\omega(x,0) = 0$. This represents the case of concentrated particle flows in which the microelements close to the wall are not able to rotate. The case corresponding to $n = \frac{1}{2}$ results in the vanishing of antisymmetric part of stress tensor and represents weak concentrations. The particle spin is equal to fluid vorticity at the boundary for the fine particle suspensions. The case corresponding to $n = 1$ is representative of turbulent boundary layer flows (Ahmadi [15], Gorla and Ameri [16]). Thus for $n = 0$, particles are not free to rotate near the surface, whereas, as n increases from 0 to 1, the microrotation term gets augmented and induces flow enhancement. In this study, the value of n is taken as 1/2 only.

In view of the continuity Eq. (1), introduce the stream function ψ by

$$u = \frac{\partial \psi}{\partial y}, v = -\frac{\partial \psi}{\partial x} \tag{7}$$

Substituting Eq. (7) in Eqs. (2)–(5) and then using the following similarity transformations

$$\left.\begin{aligned} &\xi = \frac{x}{L}, \eta = \frac{Gr_L^{1/4}}{L\xi^{1/4}}y, \psi = \frac{\mu Gr_L^{1/4}\xi^{3/4}}{\rho}f(\xi,\eta), \omega = \frac{\mu Gr_L^{3/4}\xi^{1/4}}{\rho L^2}g(\xi,\eta), \\ &\theta(\xi,\eta) = \frac{T-T_{\infty,0}}{T_w-T_{\infty,0}} - \frac{Ax}{T_w-T_{\infty,0}}, \phi(\xi,\eta) = \frac{C-C_{\infty,0}}{C_w-C_{\infty,0}} - \frac{Bx}{C_w-C_{\infty,0}} \end{aligned}\right\} \tag{8}$$

we get the following nonlinear system of differential equations.

$$\left(\frac{1}{1-N}\right)f''' + \frac{3}{4}ff'' - \frac{1}{2}(f')^2 + \left(\frac{N}{1-N}\right)g' + \theta + \mathcal{B}\phi - \frac{\xi^{1/2}}{Da_L Gr_L^{1/2}}f' - \frac{Fs}{2Da_L}f'^2 = \xi\left[f'\frac{\partial f'}{\partial \xi} - f''\frac{\partial f}{\partial \xi}\right] \tag{9}$$

$$\lambda g'' + \frac{3}{4}fg' - \frac{1}{4}f'g - \left(\frac{N}{1-N}\right)\mathcal{J}\xi^{1/2}(2g + f'') = \xi\left[f'\frac{\partial g}{\partial \xi} - g'\frac{\partial f}{\partial \xi}\right] \tag{10}$$

$$\frac{1}{\Pr}\theta'' + \frac{3}{4}f\theta' - \varepsilon_1 f' = \xi\left[f'\frac{\partial \theta}{\partial \xi} - \theta'\frac{\partial f}{\partial \xi}\right] \tag{11}$$

$$\frac{1}{Sc}\phi'' + \frac{3}{4}f\phi' - \varepsilon_2 f' = \xi\left[f'\frac{\partial \phi}{\partial \xi} - \phi'\frac{\partial f}{\partial \xi}\right] \tag{12}$$

where the primes indicate partial differentiation with respect to η alone, $Gr_L = \frac{g^*\beta_T(T_w-T_{\infty,0})L^3}{\nu^2}$ is the thermal Grashof number, $Pr = \frac{\nu}{\alpha}$ is the Prandtl number, $Sc = \frac{\nu}{D}$ is the Schmidth number, $Da_L = \frac{K_p}{L^2}$ is the Darcy number, $Fs = \frac{2bx}{L^2}$ is the Forchheimer number, $\mathcal{J} = \frac{L^2}{jGr_L^{1/2}}$ is the micro-inertia density, $\lambda = \frac{\gamma}{j\rho\nu}$ is the spin-gradient viscosity, $N = \frac{\kappa}{\mu+\kappa}$ $(0 \le N < 1)$ is the Coupling number. If $N = 0$ the flow, temperature and concentration fields are unaffected by the microstructure of the fluid and the microrotation component is a passive quantity. In this case the present problem reduces to that of a viscous fluid. $\mathcal{B} = \frac{\beta_C(C_w-C_{\infty,0})}{\beta_T(T_w-T_{\infty,0})}$ is the buoyancy ratio. Thermal buoyancy acts always vertically upwards, the species buoyancy may act in either direction depending on the relative molecular weights. So $\mathcal{B} > 0$ indicates aiding buoyancy where both the thermal buoyancy and solutal buoyancy are in the same direction and $\mathcal{B} < 0$ indicates opposing buoyancy where the solutal buoyancy is in the opposite direction to the thermal buoyancy. When $\mathcal{B} = 0$, the flow is driven by thermal buoyancy alone. $\varepsilon_1 = \frac{Ax}{T_w-T_{\infty,0}}$ and $\varepsilon_2 = \frac{Bx}{C_w-C_{\infty,0}}$ are the thermal and solutal stratification parameters and are constants.

Boundary conditions Eq. (6) in terms of f, g, θ, ϕ become

$$\eta = 0: f'(\xi,0) = 0, f(\xi,0) = \frac{-4}{3}\xi\left(\frac{\partial f}{\partial \xi}\right)_{\eta=0}, g(\xi,0) = \frac{-1}{2}f''(\xi,0)$$

$$\theta(\xi,0) = 1-\varepsilon_1, \phi(\xi,0) = 1-\varepsilon_2 \tag{13a}$$

$$\eta \to \infty: f'(\xi,\infty) = 0, g(\xi,\infty) = \theta(\xi,\infty) = \phi(\xi,\infty) = 0 \tag{13b}$$

Table 1
Comparison of results for a vertical plate with unstratified case [17].

$\overline{Nu}Gr_L^{-1/4}$		
Pr	Ming-I Char et.al. [17]	Present results
0.7	0.44600	0.44600
2.0	0.62809	0.62800
6.0	0.87825	0.87821
20.0	1.27226	1.27204

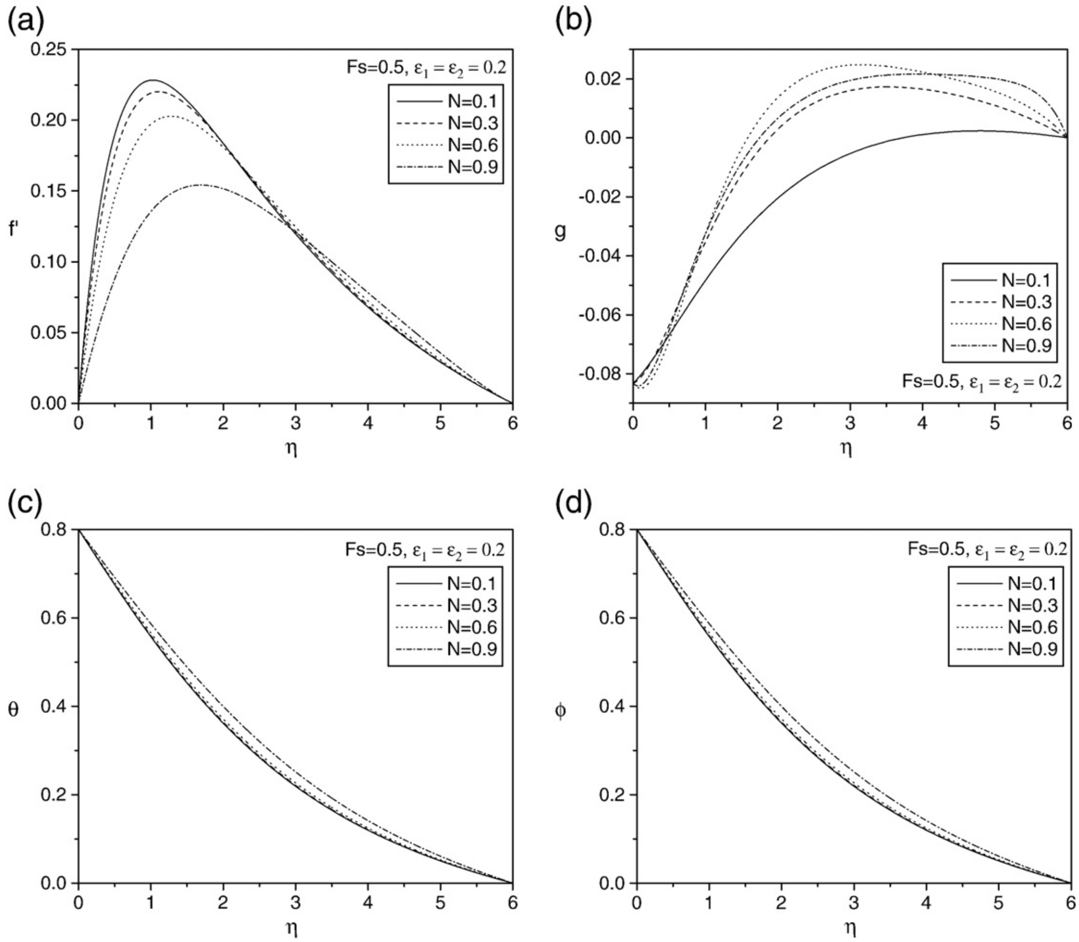

Fig. 1. (a) Velocity, (b) microrotation, (c) temperature and (d) concentration profiles for various values of *N*.

If $Da\rightarrow\infty$, $\varepsilon_1=0$ and $\varepsilon_2=0$, the problem reduces to free convection heat and mass transfer on a vertical plate with uniform wall temperature and concentration in an unstratified micropolar fluid. In the limit, as $Da\rightarrow\infty$ and $\mathcal{B}\rightarrow 0$, the governing Eqs. (2)–(5) reduce to the corresponding equations for a free convection heat transfer in a micropolar fluids. Hence, the case of the coupling of wall conduction with laminar free convection heat transfer of an unstratified micropolar fluids along a isothermal vertical flat plate of Ming et al. [17] can be obtained by taking $Da\rightarrow\infty$, $\varepsilon_1=0$, $\varepsilon_2=0$ and $\mathcal{B}=0$.

The wall shear stress and the wall couple stress are

$$\tau_w=\left[(\mu+\kappa)\frac{\partial u}{\partial y}+\kappa\omega\right]_{y=0}, \tag{14a}$$

$$m_w=\gamma\left[\frac{\partial\omega}{\partial y}\right]_{y=0} \tag{14b}$$

and the heat and mass transfers from the plate respectively are given by

$$q_w=-k\left[\frac{\partial T}{\partial y}\right]_{y=0} \tag{15a}$$

$$q_m=-D\left[\frac{\partial C}{\partial y}\right]_{y=0} \tag{15b}$$

The non-dimensional wall shear stress $C_f=\frac{2\tau_w}{\rho U_*^2}$, wall couple stress $M_w=\frac{m_w}{\rho U_*^2 L}$, the the local Nusselt number $Nu_x=\frac{q_w x}{k}$ and local Sherwood number $Sh_x=\frac{q_m x}{D}$, where U_* is the characteristic velocity, are given by

$$C_f=\left(\frac{2-N}{1-N}\right)Gr_x^{-1/4}f''(\xi,0), \tag{16a}$$

$$M_w=\left(\frac{\lambda}{\mathcal{J}}\right)\xi^{1/2}Gr_x^{-1/2}g'(\xi,0) \tag{16b}$$

$$Nu_x=-Gr_x^{1/4}\theta'(\xi,0), \tag{16c}$$

$$Sh_x=-Gr_x^{1/4}\phi'(\xi,0) \tag{16d}$$

where $Gr_x=\frac{g^*\beta_T(T_w-T_{\infty,0})x^3}{\nu^2}$ is the local thermal Grashof number.

In terms of non-dimensional variables, the average Nusselt number and Sherwood numbers are

$$\frac{\overline{Nu}}{Gr_L^{1/4}}=\int_0^1\xi^{-1/4}\theta'(\xi,0)d\xi,\frac{\overline{Sh}}{Gr_L^{1/4}}=\int_0^1\xi^{-1/4}\phi'(\xi,0)d\xi \tag{17}$$

3. Results and discussions

The flow Eqs. (9) and (10) which are coupled, together with the energy and concentration Eqs. (11) and (12), constitute nonlinear nonhomogeneous differential equations for which closed-form solutions cannot be obtained. Hence, these Eqs. (9) to (12) are solved numerically using the Keller-box implicit method discussed in Cebeci

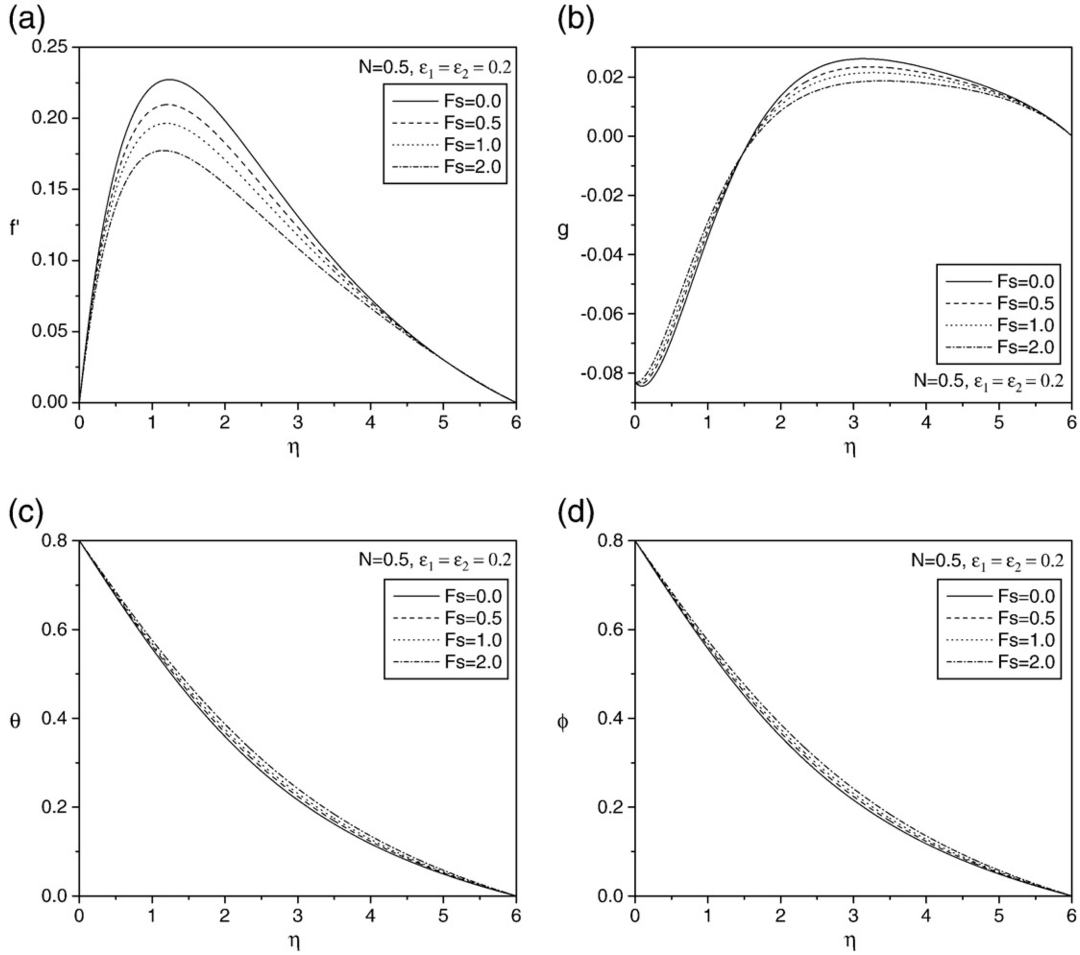

Fig. 2. (a) Velocity, (b) microrotation, (c) temperature and (d) concentration profiles for various values of *Fs*.

and Bradshaw [14]. This method has been proven to be adequate and give accurate results for boundary layer equations. In the present study the boundary conditions for η at ∞ are replaced by a sufficiently large value of η where the velocity, microrotation, temperature and concentration profiles approach zero. In the present calculations, the value of η_∞ is taken as 6 and a grid size of η as 0.02. The solutions are computed for the dimensionless velocity, microrotation, temperature and concentration and shown graphically through Figs. (1–4). In order to study the effects of the coupling number N, Forchheimer number Fs, thermal stratification parameter ε_1 and solutal stratification parameter ε_2 on the physical quantities of the flow, the remaining parameters are fixed as $\mathcal{J}=5.0$, $\lambda=5.0$, $\mathcal{B}=1.0$, $\Pr=0.7$, $Sc=0.7$, $Gr_L=10$, $Da_L=0.1$ and $\xi=0.1$. These values are chosen so as to satisfy the thermodynamic restrictions on the material parameters given by Eringen [5].

In the absence of stratification parameters ε_1 and ε_2 with $N=0.5$, $Da\to\infty$, $\mathcal{J}=50000$, $\lambda=5.0$ and $\mathcal{B}=0.0$, the results have been compared with the special case of laminar free convection flow of micropolar fluids along an isothermal vertical flat plate[17] and it is found that they are in good agreement, as shown in (Table 1).

In Fig. 1(a–d), the effects of the coupling number N on the dimensionless velocity, microrotation, temperature and concentration profiles are presented for fixed values of $Fs=0.5$ and $\varepsilon_1=\varepsilon_2=0.2$. As N increases, it can be observed from Fig. 1(a) that the maximum velocity decreases in amplitude and the location of the maximum velocity moves farther away from the wall. Since $N\to 0$ corresponds to the case of viscous fluid, the velocity in case of micropolar fluid is less that of viscous fluid. From Fig. 1(b), it can be noticed that the microrotation changes sign from negative to positive values within the boundary layer. It is clear from Fig. 1(c) that the temperature increases with the increase of coupling number N. It can be seen from Fig. 1(d) that the concentration of the fluid increases with the increase of coupling number N. The temperature and concentration in case of micropolar fluids is more than that of the corresponding Newtonian fluid case.

The dimensionless velocity component for different values of Forchheimer number Fs with $N=0.5$ and $\varepsilon_1=\varepsilon_2=0.2$ is depicted in Fig. 2(a). It shows the effects of Forchheimer (inertial porous) parameter on the velocity. In the absence of Forchheimer number (i.e., when $Fs=0$), the present investigation reduces to a natural convection heat and mass transfer in a micropolar fluid saturated with porous medium in the presence of stratification effects. An increase in Fs is seen to considerably lower velocity profiles closer to the wall and the influence is reversed away from the wall. From Fig. 2(b), it can be observed that the microrotation changes sign from negative to positive values at the critical point $\eta=1.6$ within the boundary layer. Also, it is clear that the magnitude of the microrotation decreases with an increase in Forchheimer parameter for $N=0.5$, $\varepsilon_1=\varepsilon_2=0.2$. The dimensionless temperature for different values of Forchheimer parameter for $N=0.5$ and $\varepsilon_1=\varepsilon_2=0.2$, is displayed in Fig. 2(c). It is seen that the temperature of the fluid increases with the increase of Forchheimer parameter. Fig. 2(d) demonstrates the dimensionless concentration for different values of Forchheimer parameter with $N=0.5$ and $\varepsilon_1=\varepsilon_2=0.2$. It is clear that the

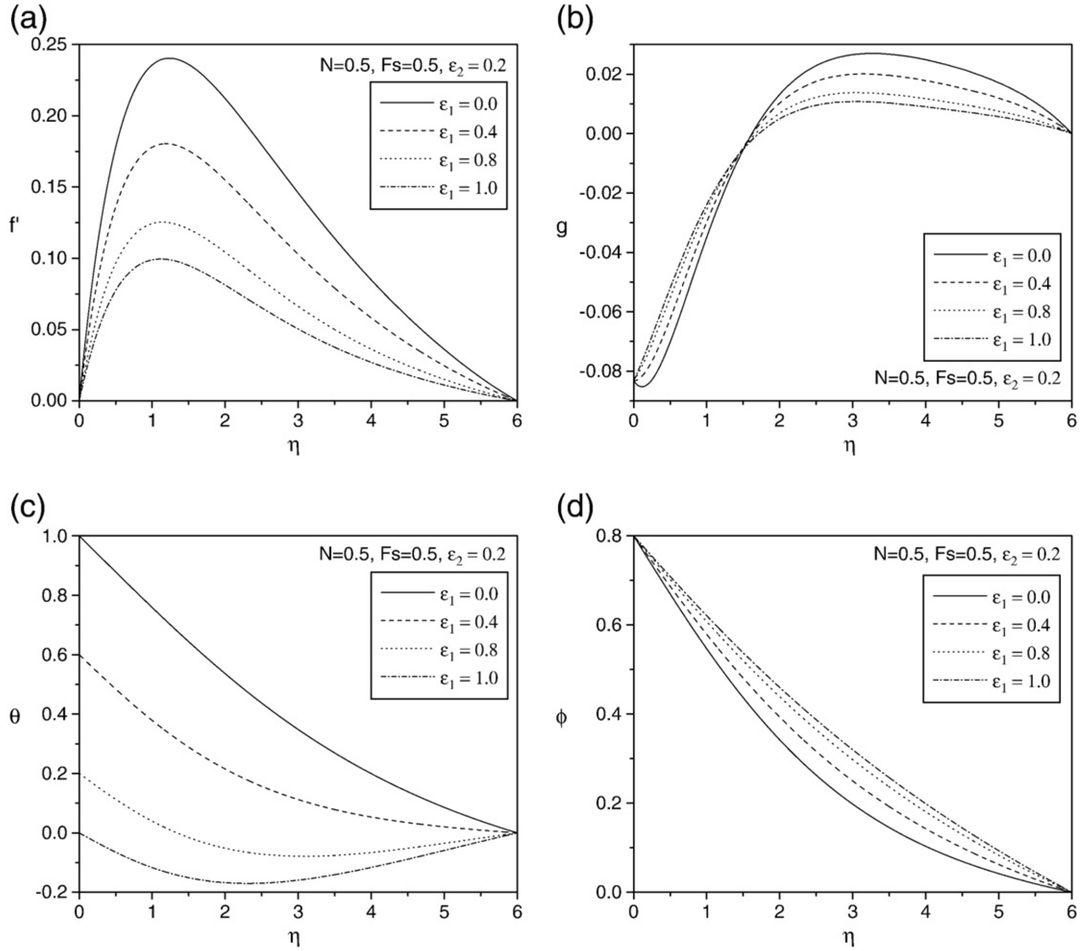

Fig. 3. (a) Velocity, (b) microrotation, (c) temperature and (d) concentration profiles for various values of ε_1.

concentration of the fluid increases with the increase of Forchheimer parameter.

Fig. 3(a) depicts the non-dimensional velocity for different values of thermal stratification parameter ε_1 for fixed values of $N=0.5$, $Fs=0.5$ and $\varepsilon_2=0.2$. It is observed that the velocity of the fluid decreases with the increase of thermal stratification parameter. From Fig. 3(b), it can be noticed that the microrotation changes sign from negative to positive values at the critical point $\eta=1.6$ within the boundary layer. Also, the magnitude of the microrotation decreases with an increase in thermal stratification parameter. The dimensionless temperature for different values of thermal stratification parameter for $N=0.5$, $Fs=0.5$ and $\varepsilon_2=0.2$, is shown in Fig. 3(c). It is clear that the temperature of the fluid decreases with the increase of thermal stratification parameter. Fig. 3(d) demonstrates the dimensionless concentration for different values of thermal stratification parameter for $N=0.5$, $Fs=0.5$and $\varepsilon_2=0.2$. It can be seen that the concentration of the fluid increases with the increase of thermal stratification parameter.

The dimensionless velocity component for different values of solutal stratification parameter ε_2 with constant $N=0.5$, $Fs=0.5$ and $\varepsilon_1=0.4$, is depicted in Fig. 4(a). It is observed that the velocity of the fluid decreases with the increase of solutal stratification parameter. From Fig. 4(b), it can be noticed that the microrotation changes sign from negative to positive values at the critical point $\eta=1.6$ within the boundary layer. Also, it is clear that the magnitude of the microrotation decreases with an increase in solutal stratification parameter for $N=0.5$, $Fs=0.5$ and $\varepsilon_1=0.4$. The dimensionless temperature for different values of solutal stratification parameter for $N=0.5$, $Fs=0.5$ and $\varepsilon_1=0.4$, is displayed in Fig. 4(c). It is seen that the temperature of the fluid increases with the increase of solutal stratification parameter. Fig. 4(d) demonstrates the dimensionless concentration for different values of solutal stratification parameter with $N=0.5$, $Fs=0.5$ and $\varepsilon_1=0.4$. It is clear that the concentration of the fluid decreases with the increase of thermal stratification parameter.

(Table 2) shows the effects of the coupling number N, Forchheimer number Fs, thermal stratification parameter ε_1 and solutal stratification parameter ε_2 on the skin friction parameter $f''(\xi,0)$ and the dimensionless wall couple stress $g'(\xi,0)$. It is observed from this table that both the skin friction parameter and the wall couple stress decrease with increasing coupling number N. The skin friction parameter decreases and the wall couple stress increases as Fs increases. Also, the skin friction parameter decreases while the wall couple stress increases as ε_1 increases. Further, the skin friction parameter decreases but the wall couple stress increases as ε_2 increases.

(Table 3) displays the effect of coupling number N on the non-dimensional heat and mass transfer coefficients with variation of the thermal stratification parameter ε_1 and solutal stratification parameter ε_2 for fixed $Fs=0.5$. It can be seen from this table that, for fixed values of N, the heat and mass transfer coefficients are decreasing with increasing values of both ε_1 and ε_2. Also, for fixed values of both ε_1 and ε_2, the heat and mass transfer coefficients are decreasing with the increasing values of coupling number N. Further, it can be noticed that the heat and mass transfer coefficients are more in case of viscous

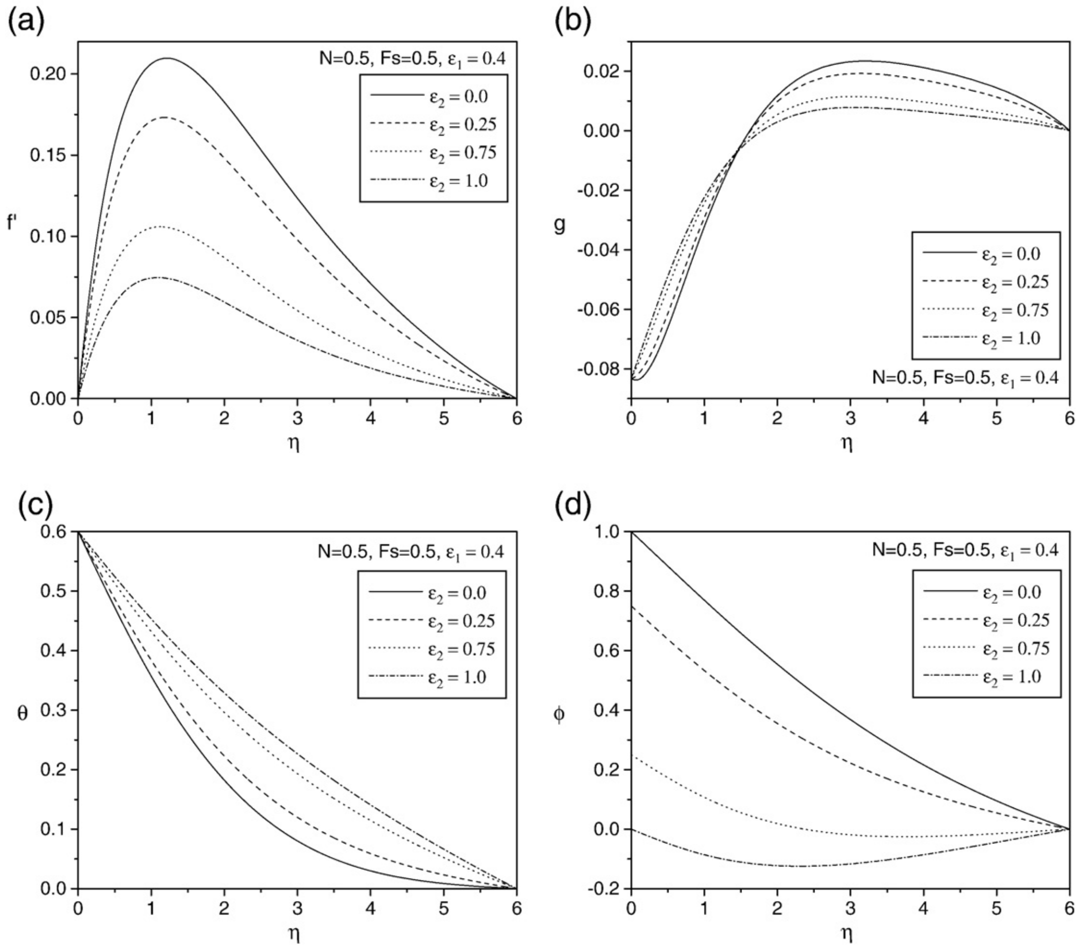

Fig. 4. (a) Velocity, (b) microrotation, (c) temperature and (d) concentration profiles for various values of ε_2.

fluids. Therefore the presence of microscopic effects arising from the local structure and micromotion of the fluid elements reduce the heat and mass transfer coefficients.

The effects of Forchheimer number *Fs* on the non-dimensional heat and mass transfer coefficients against the thermal stratification parameter ε_1 and solutal stratification parameter ε_2 is presented in (Table 4). It can be observed from this table that, for fixed values of ε_1 and ε_2, the non-dimensional heat and mass transfer coefficients are reducing with the increasing values of Forchheimer number *Fs*. Similarly for fixed values of Forchheimer number, the heat and mass transfer coefficients are decreasing with increasing value of both ε_1 and ε_2. Hence, the inertial effects in micropolar fluid saturated porous medium reduce the skin friction and couple stresses.

Table 2
Effect of skin friction and wall couple stress for various values of *N*, *Fs*, ε_1 and ε_2.

N	Fs	ε_1	ε_2	$f''(\xi,0)$	$-g'(\xi,0)$
0.1	0.5	0.2	0.2	0.6537	−0.0245
0.3	0.5	0.2	0.2	0.5713	−0.0111
0.6	0.5	0.2	0.2	0.4239	0.0352
0.9	0.5	0.2	0.2	0.2161	0.0470
0.5	0.0	0.2	0.2	0.4956	0.0272
0.5	0.5	0.2	0.2	0.4774	0.0178
0.5	1.0	0.2	0.2	0.4631	0.0106
0.5	2.0	0.2	0.2	0.4415	0.0001
0.5	0.5	0.0	0.2	0.5390	0.0374
0.5	0.5	0.4	0.2	0.4170	−0.0011
0.5	0.5	0.8	0.2	0.2994	−0.0370
0.5	0.5	1.0	0.2	0.2421	−0.0540
0.5	0.5	0.4	0.0	0.4774	0.0178
0.5	0.5	0.4	0.25	0.4020	−0.0057
0.5	0.5	0.4	0.75	0.2564	−0.0498
0.5	0.5	0.4	1.0	0.1857	−0.0705

4. Conclusions

In this paper, a boundary layer analysis for free convection flow in a doubly stratified non-Darcy micropolar fluid over a vertical plate with uniform plate temperature and concentration is presented. Using the similarity variables, the governing equations are transformed into a set of non-similar parabolic equations where numerical solution has been obtained for a wide range of parameters. The higher values of the coupling number *N* result in lower velocity distribution but higher temperature, concentration distributions in the boundary layer compared the Newtonian fluid case($N=0$). The lower velocity profiles and the higher temperature and concentration profiles occur for the higher values of Forchheimer number *Fs*. An increase in the both thermal and solutal stratification parameters, the velocity, skin friction parameter and non-dimensional heat and mass transfer coefficients are decreasing but the wall couple stress is increasing. An increase in the thermal stratification parameter, decrease the temperature but increase the concentration distribution. The reverse trend is observed for temperature and concentration distributions in case of solutal stratification parameter. The numerical results indicate that the micropolar fluids reduce the skin friction but increase the wall couple stresses. Also, non-dimensional heat and mass transfer coefficients decrease with the increasing values of the coupling number and Forchheimer number.

Table 3
Variation of non-dimensional heat and mass transfer coefficients versus ε_1 and ε_2 for different values of N with $Fs = 0.5$.

$Nu_xGr_x^{-1/4}$						$Sh_xGr_x^{-1/4}$			
ε_1	ε_2	$N=0.1$	$N=0.3$	$N=0.6$	$N=0.9$	$N=0.1$	$N=0.3$	$N=0.6$	$N=0.9$
0.0	0.3	0.3125	0.3097	0.2901	0.2463	0.3411	0.3332	0.3146	0.2627
0.2	0.3	0.3033	0.2967	0.2815	0.2413	0.3135	0.3063	0.2895	0.2439
0.4	0.3	0.2923	0.2852	0.2690	0.2255	0.2858	0.2793	0.2646	0.2256
0.6	0.3	0.2665	0.2593	0.2431	0.1996	0.2581	0.2525	0.2400	0.2080
0.8	0.3	0.2264	0.2195	0.2044	0.1643	0.2309	0.2262	0.2162	0.1912
1.0	0.3	0.1725	0.1665	0.1539	0.1204	0.2041	0.2006	0.1933	0.1752
0.2	0.0	0.3390	0.3314	0.3139	0.2654	0.3076	0.3115	0.2975	0.2516
0.2	0.2	0.3153	0.3083	0.2923	0.2492	0.3153	0.3083	0.2923	0.2492
0.2	0.4	0.2913	0.2850	0.2708	0.2334	0.3080	0.3005	0.2832	0.2359
0.2	0.6	0.2673	0.2617	0.2495	0.2182	0.2858	0.2781	0.2604	0.2123
0.2	0.8	0.2435	0.2388	0.2287	0.2036	0.2491	0.2415	0.2246	0.1790
0.2	1.0	0.2201	0.2164	0.2086	0.1897	0.1984	0.1915	0.1766	0.1368

Table 4
Variation of non-dimensional heat and mass transfer coefficients versus ε_1 and ε_2 for different values of Fs with $N=0.3$.

$Nu_xGr_x^{-1/4}$						$Sh_xGr_x^{-1/4}$			
ε_1	ε_2	$Fs = 0.5$	$Fs = 1.0$	$Fs = 1.5$	$Fs = 2.0$	$Fs = 0.5$	$Fs = 1.0$	$Fs = 1.5$	$Fs = 2.0$
0.0	0.7	0.2615	0.2537	0.2478	0.2433	0.3029	0.2844	0.2704	0.2592
0.2	0.7	0.2502	0.2423	0.2362	0.2312	0.2615	0.2480	0.2375	0.2289
0.4	0.7	0.2248	0.2179	0.2124	0.2078	0.2208	0.2116	0.2042	0.1981
0.6	0.7	0.1860	0.1808	0.1764	0.1727	0.1811	0.1754	0.1707	0.1667
0.8	0.7	0.1343	0.1311	0.1283	0.1258	0.1426	0.1396	0.1370	0.1348
1.0	0.7	0.0704	0.0690	0.0678	0.0666	0.1054	0.1043	0.1032	0.1023
0.3	0.0	0.3332	0.3129	0.2985	0.2874	0.3052	0.2947	0.2817	0.2748
0.3	0.2	0.3063	0.2901	0.2782	0.2690	0.2967	0.2825	0.2721	0.2641
0.3	0.4	0.2793	0.2668	0.2575	0.2501	0.2852	0.2712	0.2607	0.2524
0.3	0.6	0.2525	0.2434	0.2364	0.2308	0.2593	0.2469	0.2372	0.2294
0.3	0.8	0.2262	0.2200	0.2151	0.2110	0.2195	0.2095	0.2015	0.1948
0.3	1.0	0.2006	0.1968	0.1937	0.1910	0.1665	0.1594	0.1535	0.1484

References

[1] D.A. Nield, Onset of thermohaline convection in a porous medium, Water Resour. Res. 4 (3) (1968) 553–560.
[2] A.A. Khan, A. Zebib, Double diffusive instability in a vertical layer of a porous medium, J. Heat Transfer 103 (1) (1981) 179–181.
[3] V.M. Soundalgekar, Effect of mass transfer on free convective flow of a dissipative incompressible fluid past an infinite vertical porous plate with suction, Proc. Indian Acad. Sci. 84A (5) (1976) 194–203.
[4] D.A. Nield, A. Bejan, Convection in Porous Media, third ed.Springer-Verlag, New York, 2006.
[5] A.C. Eringen, Theory of micropolar fluids, J. Math. Mech. 16 (1966) 1–18.
[6] G. Lukaszewicz, Micropolar fluids — Theory and Applications, Birkhauser, Basel, 1999.
[7] D. Rees, I. Pop, Free convection boundary-layer flow of a micropolar fluid from a vertical flat plate, IMA J. Appl. Math. 61 (2) (1998) 179–197.
[8] I.A. Hassanien, A.H. Essawy, N.M. Moursy, Natural convection flow of micropolar fluid from a permeable uniform heat flux surface in porous medium, Appl. Math. Comput. 152 (2) (2004) 323–335.
[9] O. Abdulaziz, I. Hashim, Fully developed free convection heat and mass transfer of a micropolar fluid between porous vertical plates, Numer. Heat Transfer, Part A: Applications 55 (3) (2009) 270–288.
[10] P.V.S.N. Murthy, D. Srinivasacharya, P.V.S.S.S.R. Krishna, Effect of double stratification on free convection in Darcian porous medium, J. Heat Transfer 126 (2) (2004) 297–300.
[11] P.A. Lakshmi Narayana, P.V.S.N. Murthy, Free convective heat and mass transfer in a doubly stratified non-Darcy porous medium, J. Heat Transfer 128 (11) (2006) 1204–1212.
[12] O. Anwar Beg, Joaquín Zueco, H.S. Takhar, Laminar free convection from a continuously-moving vertical surface in thermally-stratified non-Darcian high-porosity medium: network numerical study, Int. Commun. Heat Mass Transfer 35 (7) (2008) 810–816.
[13] Ching-Yang Cheng, Combined heat and mass transfer in natural convection flow from a vertical wavy surface in a power-law fluid saturated porous medium with thermal and mass stratification, Int. Commun. Heat Mass Transfer 36 (4) (2009) 351–356.
[14] T. Cebeci, P. Bradshaw, Physical and Computational Aspects of Convective Heat Transfer, Springer-Verlin, New York, 1984.
[15] G. Ahmadi, Self-similar solution of incompressible micropolar boundary layer flow over a semi-infinite plate, Int. J. Eng. Sci. 14 (7) (1976) 639–646.
[16] R.S.R. Gorla, A. Ameri, Boundary layer flow of a micropolar fluid on a continuous moving cylinder, Acta Mech. 57 (3) (1985) 203–214.
[17] Ming-I Char, Cheng-Long Cheng, Effect of wall conduction on natural convection flow of micropolar fluids along a flat plate, Int. J. Heat Mass Transfer 40 (13) (1997) 3641–3652.